A Block Solver for the Exponentially Fitted IIPG-0 method

Blanca Ayuso de Dios* Ariel Lombardi† Paola Pietra ‡

Ludmil Zikatanov§

Abstract

We consider an exponentially fitted discontinuous Galerkin method and propose a robust block solver for the resulting linear systems.

1 Introduction

Let $\Omega \subset \mathbb{R}^2$ be a convex polygon, $f \in L^2(\Omega), g \in H^{1/2}(\partial\Omega)$ and let $\epsilon > 0$ be constant. We consider the advection-diffusion problem

$$-\operatorname{div}(\epsilon\nabla u - \beta u) = f \quad \text{in } \Omega, \qquad u = g \quad \text{on } \partial\Omega, \tag{1.1}$$

where $\beta \in W^{1,\infty}(\Omega)$ derives from a potential $\beta = \nabla\psi$. In applications to semiconductor devices, u represents the concentration of positive charges, ψ the electrostatic potential and the electric field $|\nabla\psi|$ might be fairly large in some parts of Ω, so that (1.1) becomes advection dominated. Its robust numerical approximation and the design of efficient solvers, are still nowdays a challenge. Exponential fitting [2] and discontinuous Galerkin (DG) are two different approaches that have proved their usefulness for the approximation of (1.1). Both methodologies have been combined in [3] to develop a new family of exponentially fitted DG methods (in primal and mixed formulation). In this note, we consider a variant of these schemes, based on the use of the Incomplete Interior Penalty IIPG-0 method and propose also an efficient block solver for the resulting linear systems.

By introducing the change of variable

$$\rho := e^{-\frac{\psi}{\epsilon}} u \tag{1.2}$$

*Centre de Recerca Matemàtica, Barcelona, Spain. bayuso@crm.cat

†Departamento de Matemática, Universidad de Buenos Aires & CONICET, Argentina. aldoc7@dm.uba.ar

‡IMATI-CNR, Pavia, Italy, pietra@imati.cnr.it

§Department of Mathematics, Penn State University, USA ltz@math.psu.edu

problem (1.1) can be rewritten as the following second order problem

$$-\nabla\cdot(\kappa\nabla\rho)=f \text{ in } \Omega,\quad \rho=\chi \text{ on } \partial\Omega\ , \tag{1.3}$$

where $\kappa := \epsilon e^{\frac{\psi}{\epsilon}}$ and $\chi := e^{-\frac{\psi}{\epsilon}}g$. An IIPG-0 approximation to (1.3) combined with a suitable local approximation to (1.2), gives rise to the EF-IIPG-0 scheme for (1.1). We propose a block solver that uses ideas from [1] to reduce the cost to that of a Crouziex-Raviart (CR) (exponentially fitted) discretization. By using Tarjan's algorithm, the associated matrix is further reduced to block lower triangular form, and a block Gauss-Siedel algorithm results in an exact solver.

To give a neat presentation, we focus on the case $\beta = \nabla\psi$ piecewise constant; ψ piecewise linear continuous, although we include some numerical results for a much more general case (cf. Test 2). Due to space restrictions, we describe the method and the solver and show some numerical results; further extensions of the method (allowing ψ to be discontinuous) and the convergence analysis of the proposed solvers will be consider somewhere else.

2 The Exponentially Fitted IIPG-0 method

Let $\mathcal{T}_h$ be a shape-regular family of partitions of Ω into triangles T and let $h = \max_{T\in\mathcal{T}_h} h_T$ with h_T denoting the diameter of T for each $T \in \mathcal{T}_h$. We assume $\mathcal{T}_h$ does not contain hanging nodes. We denote by $\mathcal{E}_h^o$ and $\mathcal{E}_h^\partial$ the sets of all interior and boundary edges, respectively, and we set $\mathcal{E}_h = \mathcal{E}_h^o \cup \mathcal{E}_h^\partial$.

Average and jump trace operators: Let T^+ and T^- be two neighboring elements, and $\mathbf{n}^+$, $\mathbf{n}^-$ be their outward normal unit vectors, respectively ($\mathbf{n}^\pm = \mathbf{n}_{T^\pm}$). Let $\zeta^\pm$ and $\boldsymbol{\tau}^\pm$ be the restriction of ζ and $\boldsymbol{\tau}$ to $T^\pm$. We set:

$$\begin{aligned} 2\{\zeta\} &= (\zeta^+ + \zeta^-), \quad [\![\,\zeta\,]\!] = \zeta^+\mathbf{n}^+ + \zeta^-\mathbf{n}^- && \text{on } E\in\mathcal{E}_h^o,\\ 2\{\boldsymbol{\tau}\} &= (\boldsymbol{\tau}^+ + \boldsymbol{\tau}^-), \quad [\![\,\boldsymbol{\tau}\,]\!] = \boldsymbol{\tau}^+\cdot\mathbf{n}^+ + \boldsymbol{\tau}^-\cdot\mathbf{n}^- && \text{on } E\in\mathcal{E}_h^o, \end{aligned}$$

and on $e \in \mathcal{E}_h^\partial$ we set $[\![\,\zeta\,]\!] = \zeta\mathbf{n}$ and $\{\boldsymbol{\tau}\} = \boldsymbol{\tau}$. We will also use the notation

$$(u,w)_{\mathcal{T}_h} = \sum_{T\in\mathcal{T}_h}\int_T uwdx \qquad \langle u,w\rangle_{\mathcal{E}_h} = \sum_{e\in\mathcal{E}_h}\int_e uwds \quad \forall\, u,w,\in V^{DG}\ ,$$

where V^{DG} is the discontinuous linear finite element space defined by:

$$V^{DG} = \left\{u\in L^2(\Omega)\ :\ u_{|_T}\ \in\ \mathbb{P}^1(T)\ \forall T\in\mathcal{T}_h\right\},$$

$\mathbb{P}^1(T)$ being the space of linear polynomials on T. Similarly, $\mathbb{P}^0(T)$ and $\mathbb{P}^0(e)$ are the spaces of constant polynomials on T and e, respectively. For each $e \in \mathcal{E}_h$ (resp. for each $T \in \mathcal{T}_h$), let $\mathcal{P}_e^0 : L^2(e) \longrightarrow \mathbb{P}^0(e)$ (resp. $\mathcal{P}_T^0 : L^2(T) \longrightarrow \mathbb{P}^0(T)$) be the L^2-orthogonal projection defined by

$$\mathcal{P}_e^0(u) := \frac{1}{|e|}\int_e u,\quad \forall\, u\in L^2(e)\ ,\quad \mathcal{P}_T^0(v) := \frac{1}{|T|}\int_T v,\quad \forall\, v\in L^2(T)\ .$$

We denote by V^{CR} the classical Crouziex-Raviart (CR) space:

$$V^{CR}=\left\{v\in L^2(\Omega)\,:\,v_{|_T}\in\mathbb{P}^1(T)\,\forall T\in\mathcal{T}_h\ \text{and}\ \mathcal{P}^0_e[\![\,v\,]\!]=0\ \forall\, e\in\mathcal{E}_h\right\}.$$

Note that $v=0$ at the midpoint m_e of each $e\in\mathcal{E}_h^\partial$. To represent the functions in V^{DG} we use the basis $\{\varphi_{e,T}\}_{T\in\mathcal{T}_h,e\in\mathcal{E}_h}$, defined by

$$\forall\, T\in\mathcal{T}_h\quad \varphi_{e,T}(x)\in\mathbb{P}^1(T)\quad e\subset\partial T\quad \varphi_{e,T}(m_{e'})=\delta_{e,e'}\quad \forall e'\in\mathcal{E}_h\,. \tag{2.1}$$

In particular, any $w\in\mathbb{P}^1(T)$ can be written as $w=\sum_{e\subset\partial T}w(m_e)\varphi_{e,T}$.

The Exponentially fitted IIPG-0 method We first consider the IIPG-0 approximation to the solution of (1.3): Find $\rho\in V^{DG}$ such that $\mathcal{A}(\rho,w)=(f,w)_{\mathcal{T}_h}$ forall $w\in V^{DG}$ with

$$\mathcal{A}(\rho,w)=(\kappa_T^*\nabla\rho,\nabla w)_{\mathcal{T}_h}-\langle\{\kappa_T^*\nabla\rho\},[\![\,w\,]\!]\rangle_{\mathcal{E}_h}+\langle S_e\{[\![\,\rho\,]\!]\},\mathcal{P}^0([\![\,w\,]\!])\rangle_{\mathcal{E}_h}\,. \tag{2.2}$$

Here, S_e is the penalty parameter and $\kappa_T^*\in\mathbb{P}^0(T)$ the harmonic average approximation to $\kappa=\epsilon e^{\psi/\epsilon}$ both defined by [3]:

$$\kappa_T^*:=\frac{1}{\mathcal{P}^0_T(\kappa^{-1})}=\frac{\epsilon}{\mathcal{P}^0_T(e^{-\frac{\psi}{\epsilon}})}\,,\qquad S_e:=\alpha_e h_e^{-1}\{\kappa_T^*\}_e\,, \tag{2.3}$$

Next, following [3] we introduce the local operator $\mathfrak{T}:V^{DG}\longrightarrow V^{DG}$ that approximates the change of variable (1.2):

$$\mathfrak{T}w:=\sum_{T\in\mathcal{T}_h}(\mathfrak{T}w)|_T=\sum_{T\in\mathcal{T}_h}\sum_{e\subset\partial T}\mathcal{P}^0_e(e^{-\frac{\psi}{\epsilon}})w(m_e)\varphi_{e,T}\quad\forall\, w\in V^{DG}\,. \tag{2.4}$$

By setting $\rho:=\mathfrak{T}u$ in (2.2), we finally get the EF-IIPG-0 approximation to (1.1):

Find $u_h\in V^{DG}$ s.t. $\mathcal{B}(u_h,w):=\mathcal{A}(\mathfrak{T}u_h,w)=(f,w)_{\mathcal{T}_h}\ \forall\, w\in V^{DG}$ with

$$\mathcal{B}(u,w)=(\kappa_T^*\nabla\mathfrak{T}u,\nabla w)_{\mathcal{T}_h}-\langle\{\kappa_T^*\nabla\mathfrak{T}u\},[\![\,w\,]\!]\rangle_{\mathcal{E}_h}+\langle S_e\{[\![\,\mathfrak{T}u\,]\!]\},\mathcal{P}^0[\![\,w\,]\!]\rangle_{\mathcal{E}_h}\,. \tag{2.5}$$

It is important to emphasize that the use of harmonic average to approximate $\kappa=\epsilon e^{\psi/\epsilon}$ as defined in (2.3) together with the definition of the local approximation of the change of variables prevents possible overflows in the computations when ψ is large and ϵ is small. (See [3] for further discussion). Also, these two ingredients are essential to ensure that the resulting method has an automatic upwind mechanism built-in that allows for an accurate approximation of the solution of (1.1) in the advection dominated regime. We will discuss this in more detail in Section 3.

Prior to close this section, we define for each $e\in\mathcal{E}_h$ and $T\in\mathcal{T}_h$:

$$\psi_{m,e}:=\min_{x\in e}\psi(x)\quad \psi_{m,T}:=\min_{x\in T}\psi(x);\quad \psi_{m,T}\le\psi_{m,e}\ \text{for}\ e\subset\partial T\,.$$

In the advection dominated regime $\epsilon\ll|\beta|h=|\nabla\psi|h$

$$\mathcal{P}^0_T(e^{-(\psi/\epsilon)})\simeq\epsilon^2e^{-\frac{\psi_{m,T}}{\epsilon}}\qquad\qquad \mathcal{P}^0_{e_i}(e^{-\psi/\epsilon})\simeq\epsilon\,e^{-\frac{\psi_{m,e}}{\epsilon}}\,. \tag{2.6}$$

The first of the above scalings together with the definitions in (2.3) implies

$$\kappa_T^*\simeq\frac{1}{\epsilon}e^{\frac{\psi_{m,T}}{\epsilon}}\,,\qquad S_e\simeq\frac{\alpha}{2\epsilon}|e|^{-1}e^{\frac{(\psi_{m,T_1}+\psi_{m,T_2})}{\epsilon}}\qquad e=\partial T_1\cap\partial T_2\,. \tag{2.7}$$

3 Algebraic System & Properties

Let A and B be the operators associated to the bilinear forms $\mathcal{A}(\cdot,\cdot)$ (2.2) and $\mathcal{B}(\cdot,\cdot)$ (2.5), respectively. We denote by $\mathbb{A}$ and $\mathbb{B}$ their matrix representation in the basis $\{\varphi_{e,T}\}_{T\in\mathcal{T}_h, e\in\mathcal{E}_h}$ (2.1). In this basis, the operator $\mathfrak{T}$ defined in (2.4) is represented as a diagonal matrix, $\mathbb{D}$, and $\mathbb{B} = \mathbb{A}\mathbb{D}$. Thus, the approximation to (1.3) and (1.1) amounts to solve the linear systems (of dimension $2n_e - n_b$; with n_e and n_b being the cardinality of $\mathcal{E}_h$ and $\mathcal{E}_h^\partial$, respectively):

$$\mathbb{A}\boldsymbol{\rho} = \boldsymbol{F}\,, \quad \text{and} \quad \mathbb{D}\boldsymbol{u} = \boldsymbol{\rho} \qquad \text{or} \qquad \mathbb{B}\boldsymbol{u} = \widetilde{\boldsymbol{F}}\,, \tag{3.1}$$

where $\boldsymbol{\rho}, \boldsymbol{u}, \boldsymbol{F}$ and $\widetilde{\boldsymbol{F}}$ are the vector representations of ρ, u and the rhs of the approximate problems. From the definition (2.4) of $\mathfrak{T}$ it is easy to deduce the scaling of the entries of the diagonal matrix $\mathbb{D} = (d_{i,i})_{i=1}^{2n_e-n_b}$.

$$\mathbb{D} = (d_{i,j})_{i,j=1}^{2n_e-n_b} \quad d_{i,i} = \mathcal{P}^0_{e_i}(e^{-\psi/\epsilon}) \simeq \epsilon\, e^{-\frac{\psi_{m,e}}{\epsilon}}\,, \quad d_{i,j} \equiv 0 \quad i \neq j\,.$$

We now revise a result from [1]:

Proposition 3.1 *Let $\mathcal{Z} \subset V^{DG}$ be the space defined by*

$$\mathcal{Z} = \left\{ z \in L^2(\Omega) \,:\, z_{|_T} \in \mathbb{P}^1(T)\ \forall T \in \mathcal{T}_h \ \text{and}\ \mathcal{P}^0_e\{v\} = 0\ \forall\, e \in \mathcal{E}_h^o \right\}.$$

Then, for any $w \in V^{DG}$ there exists a unique $w^{cr} \in V^{CR}$ and a unique $w^z \in \mathcal{Z}$ such that $w = w^{cr} + w^z$, that is: $V^{DG} = V^{CR} \oplus \mathcal{Z}$. Moreover, $\mathcal{A}(w^{cr}, w^z) = 0\ \forall\, w^{cr} \in V^{CR}$, and $\forall\, w^z \in \mathcal{Z}$.

Proposition 3.1 provides a simple *change of basis* from $\{\varphi_{e,T}\}$ to canonical basis in V^{CR} and $\mathcal{Z}$ that results in the following algebraic structure for (3.1):

$$\boldsymbol{\rho} = \begin{bmatrix} \boldsymbol{\rho^z} \\ \boldsymbol{\rho^{cr}} \end{bmatrix}, \qquad \mathbb{A} = \begin{bmatrix} \mathbb{A}^{zz} & \mathbf{0} \\ \mathbb{A}^{vz} & \mathbb{A}^{vv} \end{bmatrix}, \qquad \mathbb{B} = \begin{bmatrix} \mathbb{B}^{zz} & 0 \\ \mathbb{B}^{vz} & \mathbb{B}^{vv} \end{bmatrix}. \tag{3.2}$$

Due to the assumed continuity of ψ, $\mathbb{D}$ is still diagonal in this basis. The algebraic structure (3.2) suggests the following exact solver:

Algorithm 3.2 *Let u_0 be a given initial guess. For $k \geq 0$, and given $u_k = z_k + v_k$, the next iterate $u_{k+1} = z_{k+1} + v_{k+1}$ is defined via the two steps:*

1. *Solve $\mathcal{B}(u^z_{k+1}, w^z) = (f, w^z)_{\mathcal{T}_h} \quad \forall\, w^z \in \mathcal{Z}$.*
2. *Solve $\mathcal{B}(u^{cr}_{k+1}, w^{cr}) = (f, w^{cr})_{\mathcal{T}_h} - \mathcal{B}(u^z_{k+1}, w^{cr}) \quad \forall\, w^{cr} \in V^{CR}$.*

Next, wet discuss how to solve efficiently each of the above steps:

Step 2: Solution in V^{CR}. In [1] it was shown that the block $\mathbb{A}^{vv}$ coincides with the stiffness matrix of a CR discretization of (1.3), and so it is an s.p.d. matrix. However, this is no longer true for $\mathbb{B}^{vv}$ which is positive definite but non-symmetric.

$$\mathcal{B}(u^{cr}, w^{cr}) = (\kappa_T^* \nabla \mathfrak{T} u^{cr}, \nabla w^{cr})_{\mathcal{T}_h} \quad \forall\, u^{cr}, w^{cr} \in V^{CR}\,.$$

In principle, the sparsity pattern of $\mathbb{B}^{vv}$ is that of a symmetric matrix. Using (2.6) and (2.3), we find that the entries of the matrix scale as:

$$\mathbb{B}^{vv} = \left(b_{i,j}^{cr}\right)_{i,j}^{n_{cr}:=n_e-n_b} \qquad b_{i,j}^{cr} := \kappa_T^* \frac{|e_i||e_j|}{|T|}\, \mathbf{n}_{e_i} \cdot \mathbf{n}_{e_j} d_j \simeq e^{-\frac{(\psi_{m,e}-\psi_{m,T})}{\epsilon}} \tag{3.3}$$

Since ψ is assumed to be piecewise linear, for each T, it attains its minimum (and also its maximum) at a vertex of T, say $\boldsymbol{x_0}$ and $\psi_{m,e}$ is attained at one of the vertex of the edge e, say $\boldsymbol{x_e}$. In particular, this implies that

$$\psi_{m,e} - \psi_{m,T} \approx \nabla\psi \cdot (\boldsymbol{x_e} - \boldsymbol{x_0}) = \beta \cdot (\boldsymbol{x_e} - \boldsymbol{x_0}) = \begin{cases} 0 & \boldsymbol{x_e} = \boldsymbol{x_0} \\ |\beta| h & \boldsymbol{x_e} \neq \boldsymbol{x_0} \end{cases}$$

Hence, in the advection dominated case $\epsilon \ll |\beta| h$ some of the entries in (3.3) vanish (up to machine precision) for ϵ small; this is the automatic upwind mechanism intrinsic of the method. As a consequence, the sparsity pattern of $\mathbb{B}^{vv}$ is no longer symmetric and this can be exploited to re-order the unknowns so that $\mathbb{B}^{vv}$ can be reduced to block lower triangular form.
Notice also that for $\mathcal{T}_h$ acute, the block $\mathbb{A}^{vv}$ being the stiffness matrix of the Crouziex-Raviart approximation to (1.3), is an M-matrix. Hence, since the block $\mathbb{B}^{vv}$ is the product of a positive diagonal matrix and $\mathbb{A}^{vv}$, it will also be an M-matrix if the triangulation is acute (see [2]).

Step 1: Solution in the $\mathcal{Z}$-space. In [1] it was shown that A^{zz} is a diagonal p.d. matrix. This is also true for $\mathbb{B}^{zz}$ since it is the product of two diagonal matrices. The continuity of ψ implies

$$\mathcal{B}(u^z, w^z) = \langle S_e \mathfrak{T} [\![\, u^z \,]\!], \mathcal{P}_e^0([\![\, w^z \,]\!]) \rangle_{\mathcal{E}_h} \quad \forall\, u^z,\, w^z \in \mathcal{Z}\,. \tag{3.4}$$

Using (2.6) and (2.3) we observe that the entries of $\mathbb{B}^{zz}$ scale as:

$$\mathbb{B}^{zz} = (b_{i,j})_{i=1}^{n_e} \qquad b_{i,j} = S_{e_i}|e_i| d_j \delta_{i,j} \simeq \delta_{i,j} \frac{\alpha}{2}\, e^{-(\psi_{m,e}-\psi_{m,T_1}-\psi_{m,T_2})/\epsilon}$$

which are always positive, so in particular $\mathbb{B}^{zz}$ it is also an M-matrix.

4 Block Gauss-Siedel solver for V^{CR}-block

We now consider re-orderings of the unknowns (dofs), which reduce $\mathbb{B}^{vv}$ to block lower triangular form. For such reduction, we use the algorithm from [4] which roughly amounts

to *partitioning* the set of dofs into non-overlapping blocks. In the strongly advection dominated case the size of the resulting blocks is small and a block Gauss-Seidel method is an efficient solver. Such techniques have been studied in [5] for conforming methods. The idea is to consider the *directed* graph $\boldsymbol{G} = (\boldsymbol{V}, \boldsymbol{E})$ associated with $\mathbb{B}^{vv} \in \mathbb{R}^{n_{cr} \times n_{cr}}$; $\boldsymbol{G}$ has n_{cr} vertices labeled $\boldsymbol{V} = \{1, \ldots, n_{cr}\}$ and its set of edges *edges* $\boldsymbol{E}$ has cardinality equal to the number of nonzero entries[1] of $\mathbb{B}^{vv}$. By definition, $(i,j) \in \boldsymbol{E}$ *iff* $b^{cr}_{ij} \neq 0$. Note that in the advection dominated case, due to the nonsymmetric pattern of $\mathbb{B}^{vv}$ (caused by the built-in upwind mechanism), we may have $(i,j) \in \boldsymbol{E}$, while $(j,i) \notin \boldsymbol{E}$. Then, the problem of reducing $\mathbb{B}^{vv}$ to block lower triangular form of $\mathbb{B}^{vv}$ is equivalent to partitioning $\boldsymbol{G}$ as a union of strongly connected components. Such partitioning induces non-overlapping partitioning of the set of dofs, $\boldsymbol{V} = \cup_{i=1}^{N_b} \omega_i$. For $i = 1, \ldots, N_b$, let m_i denote the cardinality of ω_i; let $\mathbb{I}_i \in \mathbb{R}^{n_{cr} \times m_i}$ be the matrix that is identity on dofs in ω_i and zero otherwise; and $\mathbb{B}^{vv}_i = \mathbb{I}_i^T \mathbb{B}^{vv} \mathbb{I}_i$ is the block corresponding to the dofs in ω_i. The block Gauss-Seidel algorithm reads: *Let* $\boldsymbol{u}^{cr}_0$ *be given, and assume* $\boldsymbol{u}^{cr}_k$ *has been obtained. Then* $\boldsymbol{u}^{cr}_{k+1}$ *is computed via:* For $i = 1, \ldots N_b$

$$\boldsymbol{u}^{cr}_{k+i/N_b} = \boldsymbol{u}^{cr}_{k+(i-1)/N_b} + \mathbb{I}_i (\mathbb{B}^{vv}_i)^{-1} \mathbb{I}_i^T \left(\boldsymbol{F} - \mathbb{B}^{vv} \boldsymbol{u}^{cr}_{k+(i-1)/N_b} \right) . \tag{4.1}$$

As we report in Section 5, in the advection dominated regime the action of $(\mathbb{B}^{vv}_i)^{-1}$ can be computed exactly since the size of the blocks $\mathbb{B}^{vv}_i$ is small.

5 Numerical Results

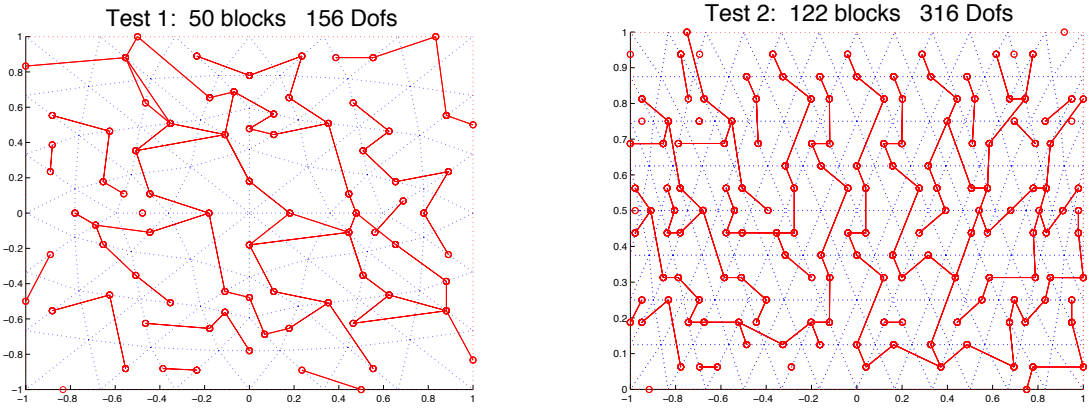

(a) Test 1 with $\epsilon = 10^{-5}$ (b) Test 2 with $\epsilon = 10^{-7}$

Figure 5.1: Plot of the connected components (blocks) of $\mathbb{B}^{vv}$ created during Tarjan's algorithm.

We present a set of numerical experiments to assess the performance of the proposed block solver. The tests refer to problem (1.3) with $\epsilon = 10^{-3}, 10^{-5}, 10^{-7}$, and Ω is triangulated with a family of unstructured triangulations $\mathcal{T}_h$. In the tables given below $J = 1$

[1] Each dof corresponds to a vertex in the graph; each nonzero entry to an edge.

corresponds to the coarsest grid and each refined triangulation on level J, $J = 2, 3, 4$ is obtained by subdividing each of the $T \in \mathcal{T}_h$ on level $(J-1)$ into four congruent triangles. From the number of triangles n_T the total number of dofs for the DG approximation is $3n_T$ and $n_e - n_b$ for the CR part of the solution.

Test 1. Boundary Layer: $\Omega = (-1, 1)^2$, $\beta = [1, 1]^t$, $n_T = 112$ for the coarsest mesh and f is such that the exact solution is given by

$$u(x, y) = \left(x + \frac{1 + e^{-2/\epsilon} - 2e^{(x-1)/\epsilon}}{1 - e^{-2/\epsilon}} \right) \left(y + \frac{1 + e^{-2/\epsilon} - 2e^{(y-1)/\epsilon}}{1 - e^{-2/\epsilon}} \right) .$$

Test 2. Rotating Flow: $\Omega = (-1, 1)^{\times}(0, 1)$, $f = 0$ and $\text{curl}\beta \neq 0$,

$$\beta = \begin{bmatrix} 2y(1 - x^2) \\ -2x(1 - y^2) \end{bmatrix}^t \quad g(x, y) = \begin{cases} 1 + \tanh\left(10(2x + 1)\right) & x \leq 0,\ y = 0, \\ 0 & \text{elsewhere} . \end{cases}$$

We stress that this test does not fit in the simple description given here, and special care is required (see [3]). For the approximation, for each $T \in \mathcal{T}_h$, with barycenter (x_T, y_T), we use the approximation $\beta|_T \approx \nabla\psi|_T$ with $\psi|_T = 2y_T(1 - x_T^2)x - 2x_T(1 - 2y_T^2)y$ (and so ψ discontinuous). The coarsest grid has $n_T = 224$ triangles.

In Figure 5.1 the plot of the connected components of the graph depicting the blocks for $\mathbb{B}^{vv}$ created during Tarjan's algorithm, on the coarsest meshes is shown; for Test 1 with $\epsilon = 10^{-5}$ and for Test 2 with $\epsilon = 10^{-7}$. In Tables 5.1 are given, the number of blocks N_b created during Tarjan's algorithm. We also report in this table the size of the largest block created (M_b maximum size) and the average size of the blocks n_{av}. Observe that in the advection dominated regime the largest block has a very small size compared to the total size of the system. After Tarjan's algorithm is used to re-order the matrix $\mathbb{B}^{vv}$, we use the block Gauss-Seidel algorithm (4.1) where each small block is solved exactly.

Acknowledgments

This work started while the first two authors were visiting the IMATI-CNR, Pavia in October 2010. Thanks go to the IMATI for the hospitality and support. The first author was partially supported by MEC grant MTM2008-03541, the second author was supported by CONICET and the fourth author is supported in part by the National Science Foundation nsf-dms 0810982.

References

[1] Blanca Ayuso de Dios and Ludmil Zikatanov. Uniformly convergent iterative methods for discontinuous Galerkin discretizations. *J. Sci. Comput.*, 40(1-3):4–36, 2009.

[2] F. Brezzi, L. D. Marini, S. Micheletti, P. Pietra, R. Sacco, and S. Wang. Discretization of semiconductor device problems. I. In *Handbook of numerical analysis. Vol. XIII*, pages 317–441. North-Holland, Amsterdam, 2005.

ϵ \ J		1	2	3	4
10^{-3}	N_b	44	150	484	1182
	M_b	23	47	95	191
	n_{av}	3.55	4.32	5.45	9.02
10^{-5}	N_b	50	210	866	3474
	M_b	23	47	95	191
	n_{av}	3.12	3.08	3.05	3.07
10^{-7}	N_b	50	210	866	3522
	M_b	23	47	95	191
	n_{av}	3.12	3.08	3.05	3.03

(a) Test 1

ϵ \ J		1	2	3	4
10^{-3}	N_b	31	1	1	1
	M_b	211	1304	5296	21344
	n_{av}	10.19	1304	5296	21344
10^{-5}	N_b	122	468	1822	7106
	M_b	4	4	7	37
	n_{av}	2.59	2.78	2.91	3.00
10^{-7}	N_b	122	468	1832	7247
	M_b	4	4	4	6
	n_{av}	2.59	2.78	2.89	2.95

(b) Test 2

Table 5.1: Number of blocks (N_b) created during the Tarjan's ordering algorithm, size of largest block (M_b) and average size of blocks (n_{av}).

[3] Ariel Lombardi and P. Pietra. Exponentially fitted discontinuous galerkin schemes for singularly perturbed problems. Technical report, IMATI-CNR, Pavia, 2010. submitted.

[4] Robert Tarjan. Depth-first search and linear graph algorithms. *SIAM J. Comput.*, 1(2):146–160, 1972.

[5] Feng Wang and Jinchao Xu. A crosswind block iterative method for convection-dominated problems. *SIAM J. Sci. Comput.*, 21(2):620–645, 1999.